ChemComm

Accepted Manuscript

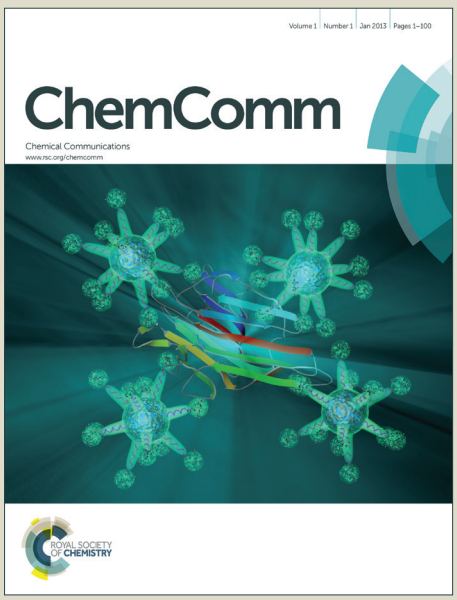

ROYAL SOCIETY OF CHEMISTRY

www.rsc.org/chemcomm

Journal Name

RSCPublishing

COMMUNICATION

Hierarchical Porous Metal-Organic Framework Monoliths

Cite this: DOI: 10.1039/xoxxoooooox

Adham Ahmed,[a] Mark Forster,[a] Rob Clowes,[a] Peter Myers[a] and Haifei Zhang*[a]

Received ooth January 2012,
Accepted ooth January 2012

DOI: 10.1039/xoxxoooooox

www.rsc.org/

Hierarchical porous crystalline metal-organic framework (MOF) monoliths are prepared by powder-packing synthesis. The resulting MOF monolithic column shows fast and efficient chromatographic separation.

MOFs are typically crystalline microporous materials formed by metal ions or clusters linked with organic ligands.[1] Introduction of larger pores such as mesopores or macropores into MOFs is desirable to enhance mass transport, which is highly important for many applications. Recent studies on enlarging MOF micropores have focused on the formation of mesoporous MOFs, by using larger ligands or ligand exchange. The mesopores formed are normally in the range of 2-10 nm.[2] Another widely used approach is to combine MOF synthesis with surfactant templating.[3] A cooperative effect between surfactant and additional agent is often necessary for the formation of mesopores. In the surfactant templating approach, the mesopores are present in addition to the micropores, while in the approach using larger ligands the normal micropores of MOFs are enlarged to mesopores.

Macropores can be formed in MOF aerogel or mechanochemical-synthesized MOFs.[4] There are intensive studies recently on macroporous MOFs, mostly in the format of colloids, capsules, powders with sponge structure, or thin films.[5] Monoliths can offer certain advantages including robustness, easy handling, low flow resistance, and essential supports for catalysis & separation applications.[6] MOFs are mostly generated as thin films or powder. The powders can be compressed to form monoliths prepared.[7] Apart from this, the preparation of MOF monoliths has been seldom reported although there are reports on the production of MOF composite including MOF-polymer monoliths.[8] For instance, direct growth and secondary seeded growth of MOFs in silica or cordierite monoliths can produce the composite monoliths, giving rise to advantages of both MOFs and monoliths.[6,8] MOF-polymer composite monoliths are prepared and used for chromatographic applications.[9] Pure MOF monoliths hold advantages over composite MOF monoliths for applications that utilize or rely on the MOF properties, *e.g.*, gas adsorption.[7] To the best of our knowledge, there has been no report on the direct synthesis of MOF monoliths from their precursors, which may offer better control on the structure and porosity of the monoliths. Here, we report the preparation of pure crystalline phase MOF monolith (*i.e.*, not composite) with a hierarchical pore structure containing micropores, mesopores and macropores via powder-packing synthesis. The presence of macropores may be particularly useful in improving mass transport for applications involving liquid phase.[10] HKUST-1 ($Cu_3(BTC)_2$, BTC is 1,3,5-benzenetricarboxylic acid) is used as a model MOF to demonstrate the methodology.

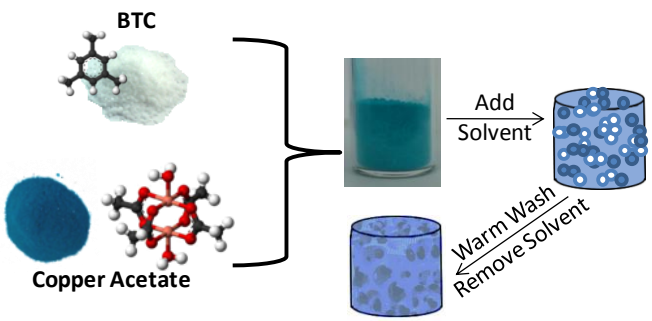

Scheme 1. Precursor powders are mixed and packed and followed by adding solvent dropwise to synthesize HKUST-1 monolith.

Scheme 1 describes how the monolith is produced. Briefly, $Cu(CH_3COO)_2 \cdot H_2O$ and BTC powders were intimately mixed together and then a small amount of ethanol was added dropwise, allowing the solvent to be fully absorbed before adding further drops. After testing several solvents (Table S1-S2,), a mixture of ethanol-water (3:4 v/v) was used for further study. The monoliths with nanoparticle-aggregated macroporous structure could be formed at the reaction temperatures of 25 – 120 ^oC (Fig. S1). White spots were observed in the as-prepared monoliths, indicating the presence of unreacted BTC. Due to larger BTC particle sizes (Fig. S2) and inefficient powder mixing, it was reasonable to suggest that not all BTC and $Cu(CH_3COO)_2$ were homogeneously converted to

HKUST-1. Grinding BTC and $Cu(CH_3COO)_2•H_2O$ powders separately (to avoid the mechanochemical reaction) using a pestle and mortar for about 1 minute could reduce the particle sizes and hence to form monoliths with improved PXRD patterns.

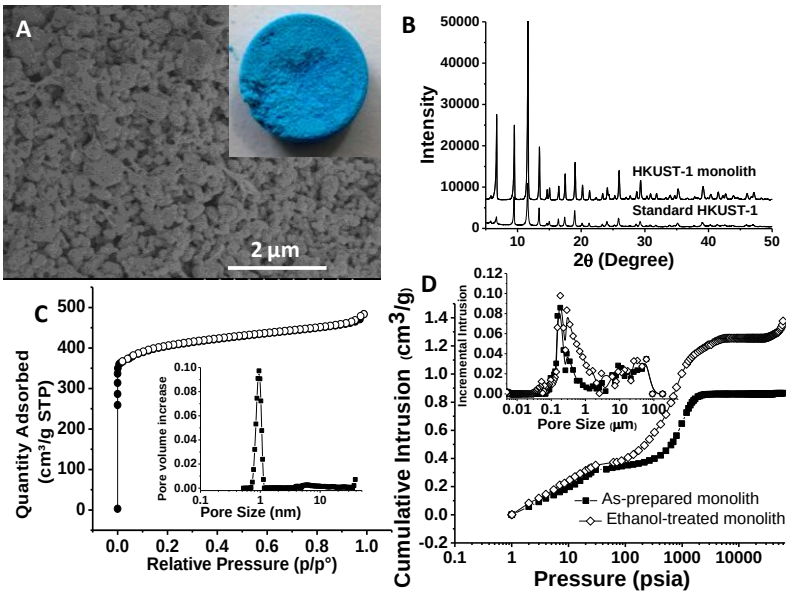

Fig. 1 Characterization of the HKUST-1 monoliths prepared by powder-packing synthesis. (A) The macroporous structure and the photo of the monolith (inset). (B) PXRD patterns of the monolith compared to the standard HKUST-1 crystals. (C) The N_2 sorption isotherm and pore size distribution, calculated by the non-local density functional theory (NLDFT). (D) The Hg intrusion cumulative curves and macropore size distribution (inset).

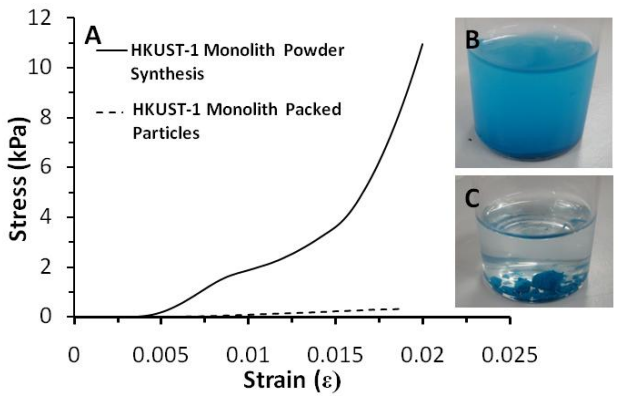

Fig. 2. (A) Comparing mechanical stability of the synthesized monolith and the pre-formed HKUST-1 particles packed monolith by compression test. Photos to show the state of the monoliths after soaking and sonication in ethanol (B) packed monolith and (C) synthesized monolith.

To produce a pure crystalline material, the as-prepared monolith at room temperature was washed/soaked in ethanol at 120 °C for 24 h. This was to remove unreacted impurities, increase porosity, and further react to improve the crystalline phase. A mass loss of 0.17 % was recorded, suggesting a high yield of HKUST-1 monolith formed. The stable monolith with interconnected macropore structure is observed (Fig. 1A). This monolith consists of aggregated particles around 300 nm. The powder X-ray diffraction (PXRD) pattern is of HKUST-1 structure (Fig. 1B). The N_2 sorption isotherm shows a microporous material profile with a sharp micropore peak around 1 nm (typical of HKUST-1, Fig.1C). As expected for the particles-aggregated monolith, a broad distribution of mesopores is observed (Fig. S3). The treated monolith shows a surface area of 1240 m^2 g^{-1} with a micropore volume of 0.561 cm^3 g^{-1} and a mesopore volume of 0.274 cm^3 g^{-1}. Further analysis by Hg intrusion porosimetry shows a high intrusion volume of 1.38 cm^3 g^{-1} with bimodal macropores around 0.2 µm and 30 µm (intrusion volume 0.86 cm^3 g^{-1} for the as-prepared monolith) (Fig.1D). Thus, Figure 1 clearly demonstrates the fabrication of MOF monoliths with interconnected micropores, mesopores, and macropores, without the need to use binders, compression or extrusion processes as commonly employed for shaping such materials into monoliths.

The MOF monoliths reported here is not a single crystalline phase, but aggregation of MOF nanocrystals. This is common for different types of monoliths reported in literature.[11] Different from physically stacked nanocrystals, these aggregated particles could offer relatively high stability for a monolith. Fig. 2A shows the higher mechanical stability by compression test of the monolith prepared using the powder-packing synthesis, compared to the monolith formed by packing pre-formed HKUST-1 particles into a column. Indeed, the Young modulus of the synthesized monolith is more than 10 times higher (442 KPa vs 38 KPa). After soaking in ethanol for 24 hours, the packed monolith was still stable. However, it turned into a fine particle suspension if further sonicated for 1 minute (Fig. 2B), while large blocks were still observed for the synthesized monolith (Fig. 2C). It was possible to form a piece of stable monolith (a disc with a diameter of 1 cm) by compression using a manual hydraulic press at pressure of 566 MPa. The monolith formed exhibited a high stability (Fig. S4). However, there was a dense skin surface and cracks developed on surface (Fig. S5). This would lead to non-uniform pore size distribution which is detrimental for monolithic applications.[11] This shows the advantages of the MOF monoliths prepared in this study over the MOF monoliths produced by powder densification.[7]

One of the emerging applications in MOFs is as stationary phase in a column for liquid phase separation.[12] Due to wide size distribution and irregular shapes of MOF crystals, packing the MOF particles into a column is not trivial, often leading to low column efficiency. MOF particles are often ground to improve the packing, but unfavorably resulting in highly increased back pressure, which in turn may crush the MOF particles. A MOF monolith fitting into a column could potentially address this problem.[13] Particularly, the presence of macropores within MOF monolith can considerably improve mass transport when liquid phase is involved. The monolithic column (Fig. 3A inset photos) was evaluated for high performance liquid chromatography (HPLC) separation. Fast separation of ethylbenzene and styrene within 2 minutes has been demonstrated with a back pressure of 134 bar (Fig. 3A). This is a significant improvement when compared to the HKUST-1 particles (Basolite C300) packed column, where only one broad peak eluted after 10 minutes (Fig. S6). In a previous study the separation was achieved with HKUST-1 packed column by liquid chromatography, but using a very long time of 150 minutes with two broad peaks.[14] Similarly a fast separation of *o*-xylene, *p*-nitrophenol and thiophene (which are industrially important) was realized in one minute (Fig. 3B). This fast separation with high resolution may be attributed to the enhanced mass transport resulted from the highly interconnected macropores in the HKUST-1 monolith.[15] The minimum pore sizes of >6 nm are required for liquid chromatography.[16] The intrinsic micropores within the HKUST-1 framework are too small for such separation. The improved separation in the macroporous monolith

occurs on the macropore surface, due to the interaction of analytes with the stationary phase (*e.g.*, π-π interaction) [14] and fast flow dynamics of the mobile phase through the macropores. The monolithic column was stable and could be used for at least 6 weeks and over 60 injections for different test mixtures. The column stability was also assessed by pumping through a mobile phase with one end open and no frit fitted at a back pressure of 300 bars. The columns was not broken and not popped out.

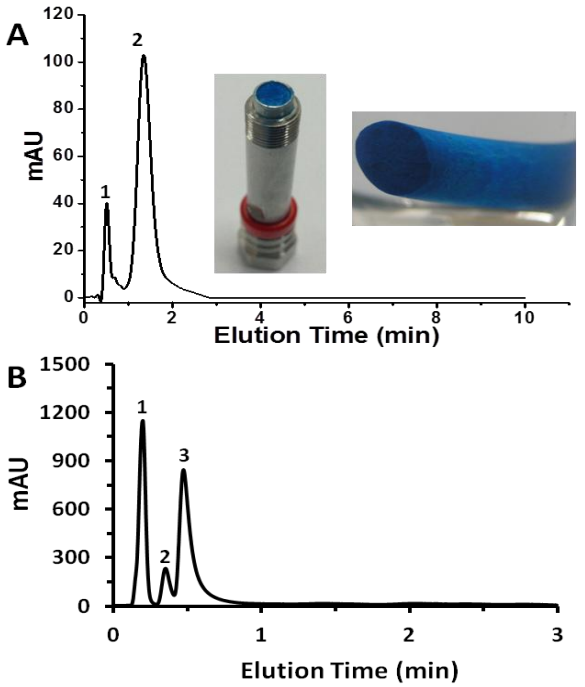

Fig. 3. (A) The HPLC chromatogram for separation of ethylbenzene (1), and styrene (2). The inset photo shows the HKUST-1 monolith in a 4.6 mm x 50 mm column and being taken out. Mobile phase heptane:dichloromethane 98:2 v/v (B) The chromatogram for the separation of o-xylene (1), p-nitrophenol (2) and thiophene (3) using the same column. Mobile phase heptanes:isopropyl alcohol 85:15 v/v. The same flow rate 1 cm^3 min^{-1} and injection volume 1 µL.

In conclusion, we have demonstrated the preparation of hierarchically porous HKUST-1 monolith with interconnected macropores by a powder-packing synthesis approach. The HKUST-1 monoliths exhibit the intrinsic micropores, additional mesopores and particularly macropores, as evidenced by N_2 sorption and Hg intrusion porosimetry. The macroporous HKUST-1 monolith is highly stable in a column. The monolithic column is demonstrated for the fast HPLC separation of ethylbenzene and styrene within 2 minutes. The methods reported here may be extended to other materials. For example, the powder-packing synthesis may be extended to prepare macroporous MIL-101 (Cr) monolith (Fig. S7). Considering the variety of MOFs, this preparation method may produce porous MOF monoliths with great potential for separation and flow catalysis.

Notes and references

[a] Department of Chemistry, University of Liverpool, Oxford Street, Liverpool, L69 7ZD. Email: zhanghf@liv.ac.uk

Electronic Supplementary Information (ESI) available: Experimental details, additional tables, SEM images, HPLC graphs, PXRD and gas sorption data, etc. See DOI: 10.1039/c000000x/

1 H.-C. Zhou, J.R. Long and O.M. Yaghi, *Chem. Rev.* 2012**, 112**, 673.
2 S. Wang, S. Ma, D. Sun, S. Parkin and H.-C. Zhou, *J. Am. Chem. Soc.* 2006, **128**, 16474; N. Klein, I. Senkovska, K. Gedrich, U. Stoeck, A. Henschel, U. Mueller and S. Kaskel, *Angew. Chem. Int. Ed.* 2009, **48**, 9954; T. Li, M.T. Kozlowski, E.A. Doud, M.N. Blakely and N.L. Rosi, *J. Am. Chem. Soc.* 2013, **135**, 11688.
3 L.-G. Qiu, T. Xu, Z.-Q. Li, W. Wang, Y. Wu, X. Jiang, X.-Y Tian and L.-D. Zhang, *Angew. Chem. Int. Ed.* 2008, **47**, 9487; Y. Zhao, J. Zhang, B. Han, J. Song and J. Li, Q. Wang, *Angew. Chem. Int. Ed.* 2011, **50**, 636; L. Sun, J. Li, J. Park and H.-C. Zhou, *J. Am. Chem. Soc.* 2012, **134**, 126.
4 M. Klimakow, P. Klobes, A.F. Thünemann, K. Rademann and F. Emmerling, *Chem. Mater.* 2010, **22**, 5216; L. Li, S. Xiang, S. Cao, J. Zhang, G. Ouyang, L. Chen and C.-Y. Su, *Nature Commun.* 2013, **4**, 1774; M.R. Lohe, M. Rose and S. Kaskel, *Chem. Commun.* 2009, 6056.
5 R. Ameloot, F. Vermoortele, W. Vanhove, M.B.J. Roeffaers, B.F. Sels and D. De Vos, *Nature Chem.* 2011, **3**, 382; J. Huo, M. Marcello, A. Garai and D. Bradshaw, *Adv. Mater.* 2013, **25**, 2717; M. Pang, A.J. Cairns, Y. Liu, Y. Belmabkhout, H.C. Zeng and M. Eddaoudi, *J. Am. Chem. Soc.* 2013, **135**, 10234; H.J. Lee, W. Cho and M. Oh, *Chem. Commun.* 2012, **48**, 221; A. Carné-Sánchez, I. Imaz, M. Cano-Sarabia and D. Maspoch, *Nature Chem.* 2013, **5**, 203; K.M. Choi, H.J. Jeon, J.K. Kang and O.M. Yaghi, *J. Am. Chem. Soc*. 2011, **133**, 11920; Y. Wu, F. Li, W. Zhu, J. Cui, C. Tao, C. Lin, P.M. Hannam and G. Li, *Angew. Chem. Int. Ed.* 2011, **50**, 12518.
6 P. Küsgens, A. Zgaverdea, H.-G. Fritz, S. Siegle and S. Kaskel, *J. Am. Ceram. Soc.* 2010, **93**, 2476; J. A. Moulijn and F. Kapteijn, *Curr. Opin. Chem. Eng.* 2013, **3**, 346.
7 J. J. Purewal, D. Liu, J. Yang, A. Sudik, D. J. Siegel, S. Maurer and U. Müller, *Int. J. Hydrogen Energy* 2012, **37**, 2723; R. Zacharia, D. Cossement, L. Lafi and R. Chahine, *J. Mater. Chem.* 2010, **20**, 2145; O. Ardelean, G. Blanita, G. Borodi, M. D. Lazar, I. Misan, I. Goldea and D. Lupu, *Int. J. Hydrogen Energy* 2013, **38**, 7046.
8 Q.-L. Zhu, Q. Xu, *Chem. Soc. Rev.* 2014, **43**, 5468; A. Sachse, R. Ameloot, B. Coq, F. Fajula, B. Coasne, D. De Vos and A. Galarneau, *Chem. Commun.* 2012, **48**, 4749; E.V. Ramos-Fernandez, M. Garcia-Domingos, J. Juan-Alcaniz, J. Gascon and F. Kapteijn, *Appl. Catal. A* 2011, **39**, 1261; T. Granato , F. Testa and R. Olivo, *Micropor. Mesopor.Mater.*2012, **153**, 236.
9 H.-Y. Huang, C.-L. Lin, C.-Y. Wu, Y.-J. Cheng and C.-H. Lin, *Anal. Chim. Acta* 2013, **779**, 96; Y. Fu, C. Yang and X. Yan, *Chem. Commun.* 2013, **49**, 7162.
10 Y. Li, Z. Fu and B. Su, *Adv. Funct. Mater.* 2012, **22**, 4634; S. Dutta, A. Bhaumik, K. C.-W. Wu, *Energy Environ. Sci.* 2014, Doi: 10.1039/C4EE01075B.
11 F. Svec, *J. Sep. Sci.* 2004, **27**, 747; M. Antonietti, N. Fechler and T. Fellinger, *Chem. Mater.* 2014, **26**, 196.
12 Z. Gu, C. Yang, N. Chang and X. Yan, *Acc. Chem. Res.* 2012, **45**, 734.
13 A. Ahmed, P. Myers and H. Zhang, *Anal. Methods.* 2012, **4**, 3942.
14 R. Ahmad, A.G. Wong-Foy and A.J. Matzger, *Langmuir* 2009, **25**, 11977.
15 A. Ahmed, N. Hodgson, M. Barrow, R. Clowes, C.M. Robertson, A. Steiner, P. McKeown, D.Bradshaw, P. Myers and H. Zhang, *J. Mater. Chem. A* 2014, **2**, 9085.
16 K.K. Unger, R. Skudas and M.M.J. Schulte , *Chromatogr. A* 2008, **1184**, 393.